Regularized Gaussian Functional Connectivity Network with Post-Hoc Interpretation for Improved EEG-based Motor Imagery-BCI Classification

Daniel Guillermo García Murillo
dggarciam@unal.edu.co

Universidad Nacional de Colombia
Signal Processing and Recognition Group - SPRG
Advisor: Andrés Marino Álvarez-Meza, Ph.D.
Co-advisor: César Germán Castellanos-Domíguez, Ph.D.

September 17, 2024

Outline I

Brain computer interface (BCI)

BCI provides people with external world communication by translating brain signals. [Khan et al., 2020]

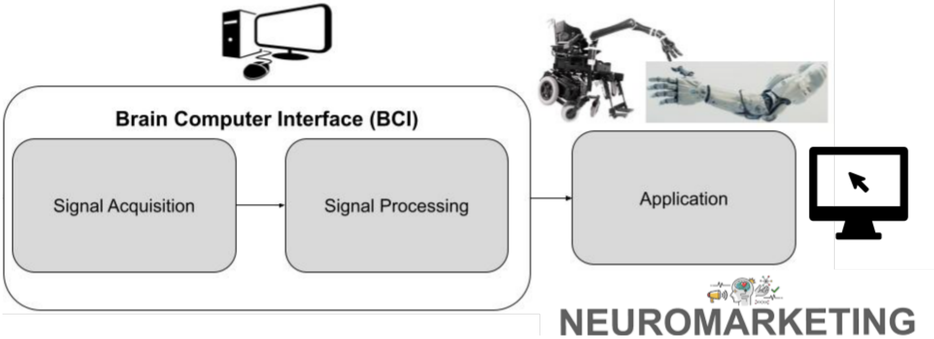

Socioeconomic facts

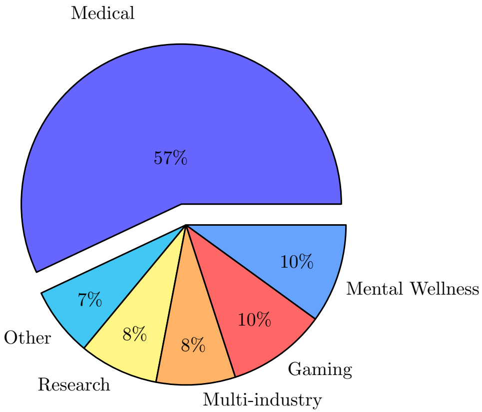

- Over 150 companies specializing in BCI as of 2019.
- BCI market valued at 228 million in 2019, projected to reach 460 million by 2029 [2].

[1] **Image:** Adapted from The World Economic Forum 2024
[2] Global Brain Computer Interface Market Research Report 2023

Motor Imagery (MI)

MI is a widely studied BCI paradigm that allows external motor communication [Cattan et al., 2018].

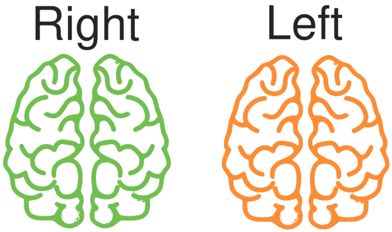

Applications:

- Recovery of motor functionality [Bonci et al., 2021].
- Motor rehabilitation [Sitaram et al., 2017].
- Virtual reality [Cattan et al., 2018].
- Gaming [Ahn et al., 2014].
- Skill acquisition [Casimo et al., 2017].

Neuroimaging techniques

- MI involves fast-evolving cognitive processes [Vărbu et al., 2022]
- EEG and MEG have remarkable temporal precision [Alsharif et al., 2020]
- EEG is portabile and cost-effective [Janapati et al., 2023, Hosseini et al., 2020]

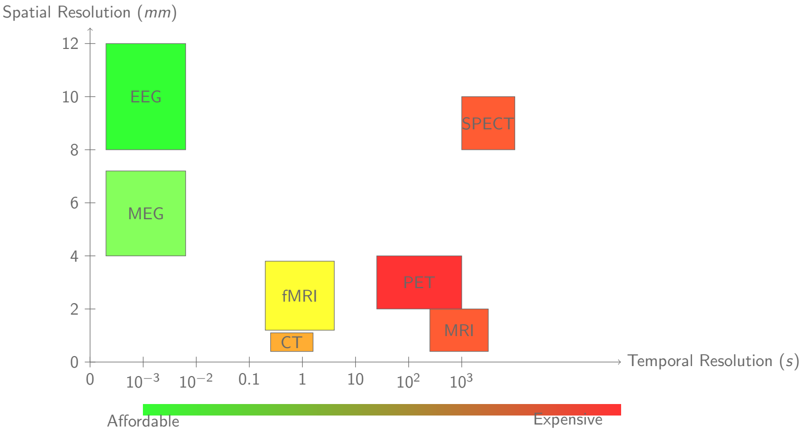

Experimental setup for MI-based BCIs

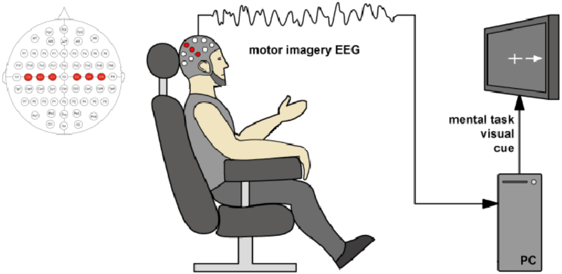

- EEG headsets are equipped with 1 to 256 electrodes [Grigorev et al., 2021].
- Visual cues are often used to guide MI tasks during EEG recordings [Hosseini et al., 2020].

[1] **Image:** Adapted from [Grigorev et al., 2021]

Sensorimotor rhythms (SMRs)

- EEG signals contains multiple electrical variations (rhythms) [Barios et al., 2019].
- Sensorimotor Rhythms (SMRs) occur in the brain's sensorimotor cortex [Altaheri et al., 2023].
- SMRs contain spectral-spatio-temporal patterns of MI tasks [Li et al., 2019].

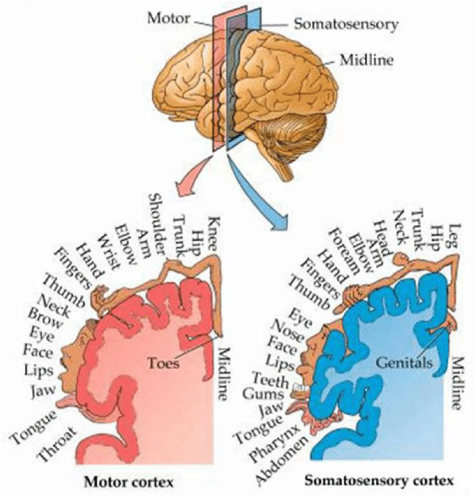

[1] **Image:** Adapted from [Purves, 2001]

MI-EEG feature extraction

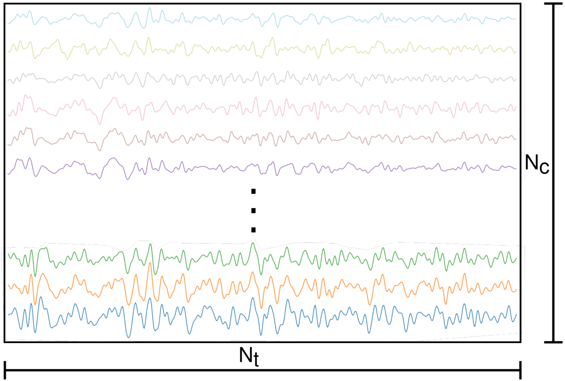

- High number of channels and sampling rate [Chevallier et al., 2024].
- Huge number of data points [Singh et al., 2021].
- Feature extraction strategies are required to reduce dimentionality [Ai et al., 2019].

Single channel feature extraction

- Capture rhythms on specific EEG channels [Samuel et al., 2017].
- Time domain: statistical [Hamedi et al., 2014], Hjorth [Yilmaz et al., 2018], etc.
- Spetral domain: Power spectral density [Oikonomou et al., 2017], Welch's periodigram [Roy et al., 2022], spectral entropy [Sarraf, 2017], etc.

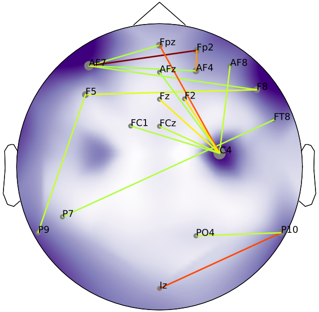

Executing or imagining motor tasks activates multiple brain areas, patterns that single-channel features fail to capture [Chiarion et al., 2023].

Multi channel feature extraction

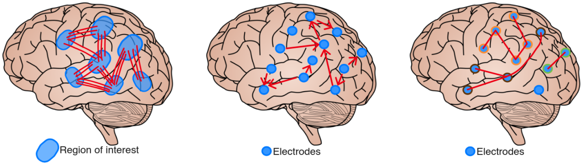

(a) Structural connectivity (b) Effective connectivity (c) Functional connectivity

- Structural connectivity (SC) focuses on physical connections, fails to capture short-living events [Thiebaut de Schotten et al., 2020]
- Effective connectivity (EC) describes direct connections and requires deep cognitive process understanding to select the best causal model [Chiarion et al., 2023].
- Functional connectivity (FC) can describe directed or non-directed connectives usually via statistical correlation [Cao et al., 2022a]

FC's simplicity, low computational demands, and lack of rigid assumptions make it ideal for MI-BCI applications [He et al., 2019].

Signal Processing and Recognition Group - SPRG

The SPRG has been working on the design of ML and DL models to improve the performance and explainability of EEG-based MI-BCIs [Collazos-Huertas et al., 2023].

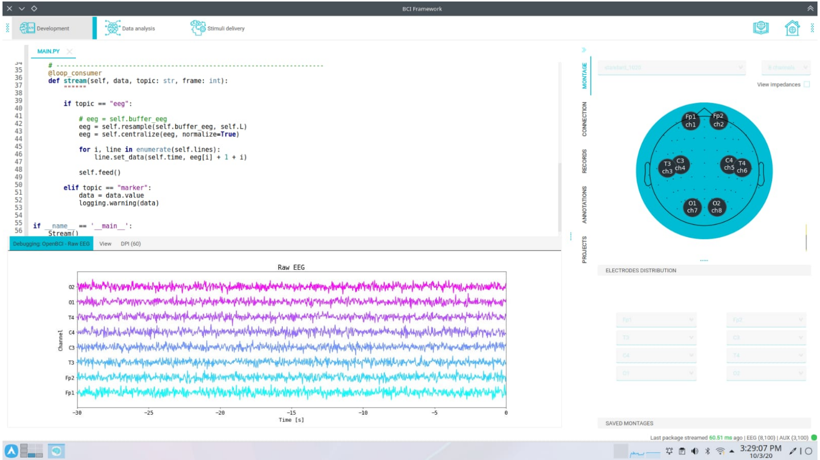

Outline I

Problem statement

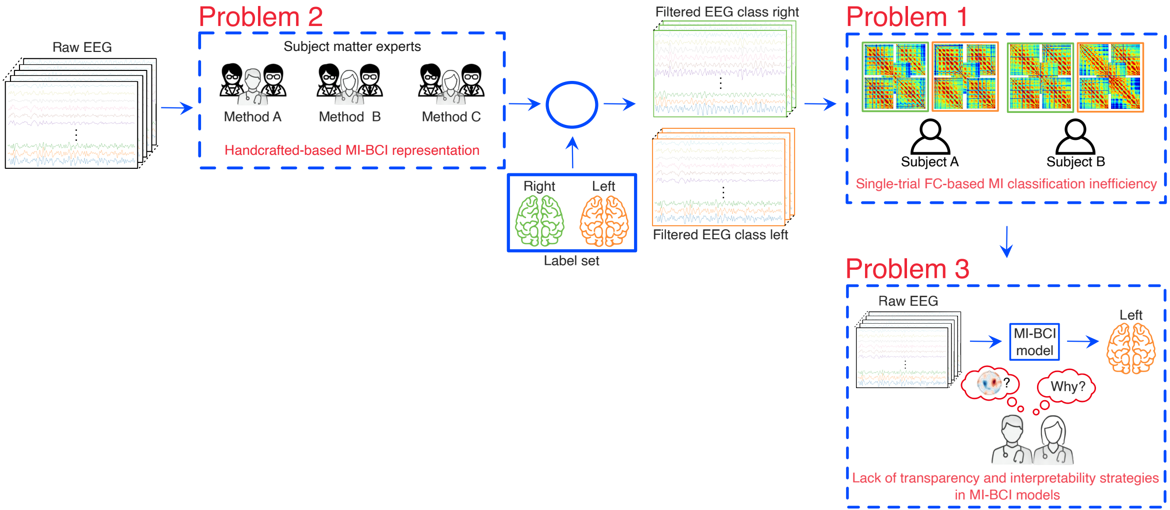

Single-Trial FC MI Classification Inefficiency

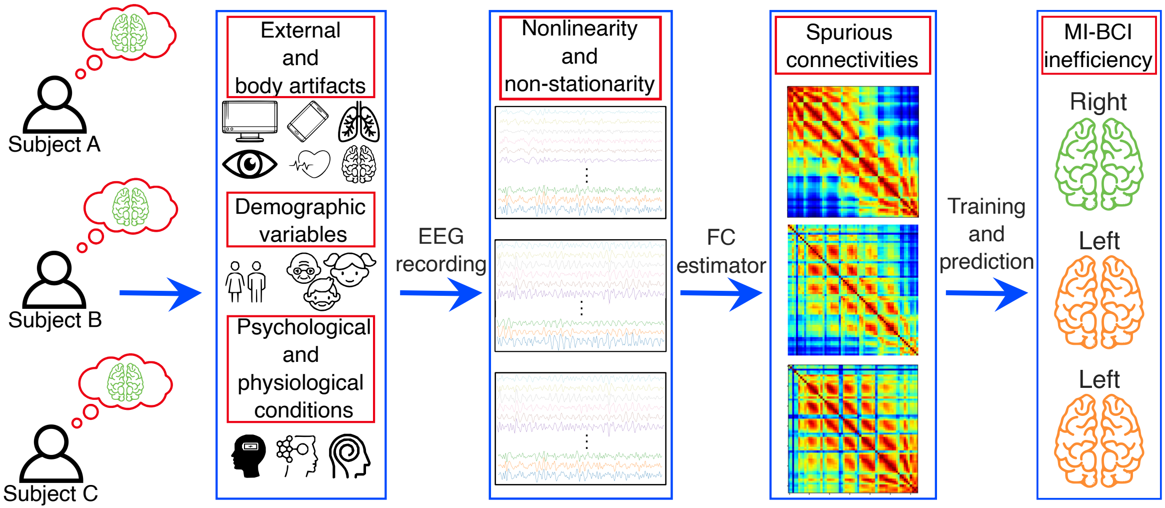

Handcrafted-based Subject-Specific EEG-based MI-BCI Representation

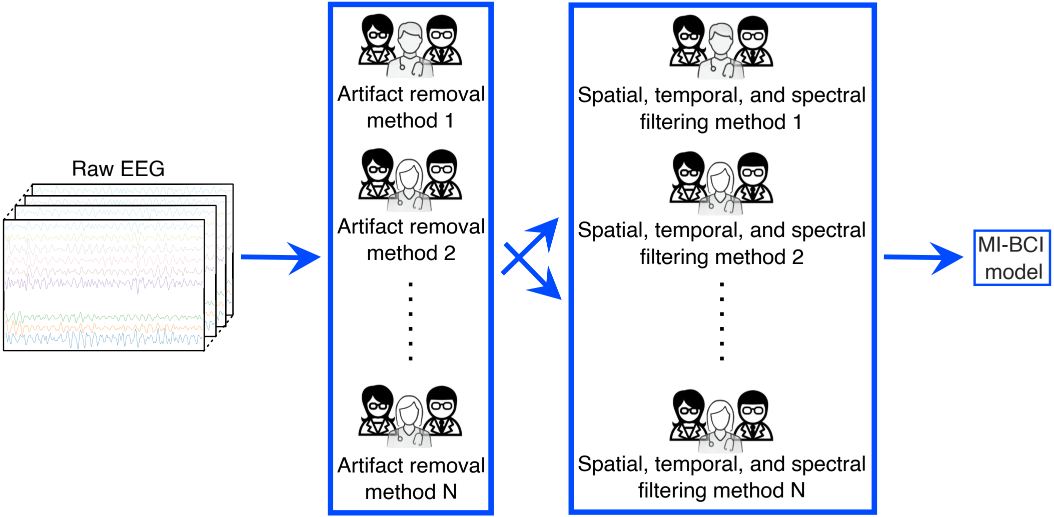

Lack of Transparency and Interpretability Strategies in MI-BCI

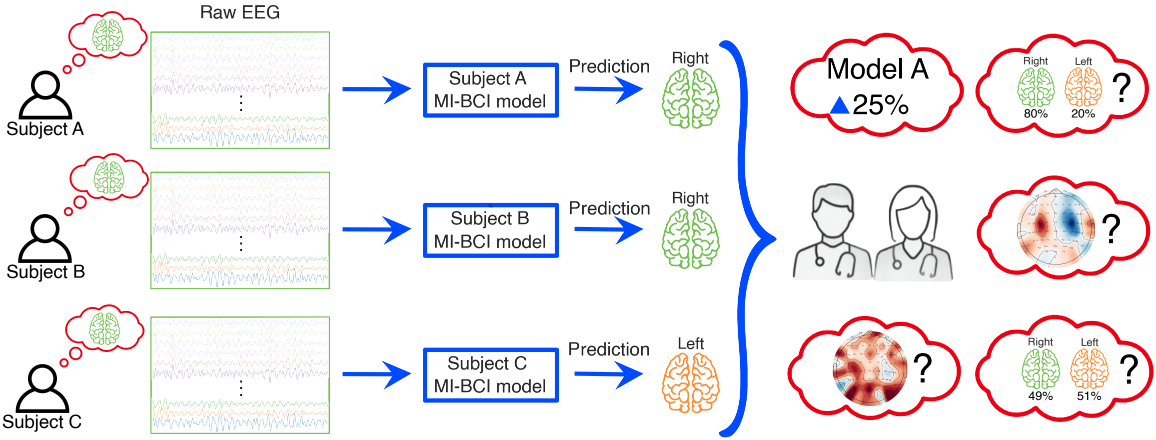

Research question

How can a single-trail FC be developed to manage non-stationary EEG subject-specific representations, handle spurious connectivities, and encode non-linear spatial, temporal, and spectral discriminative and interpretable MI patterns?

Outline I

Outline I

Functional Connectivity Estimators

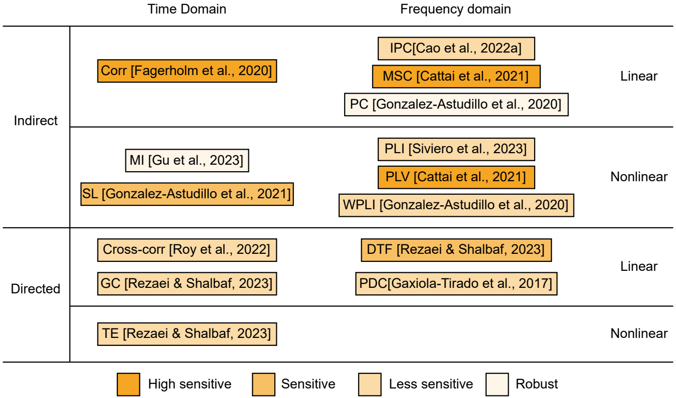

- Orange shades indicate sensitivity to volume conduction (VC).
- Linear estimators are simple but may miss complex interactions, nonlinear ones capture them but are noise-sensitive [Gonzalez-Astudillo et al., 2020].
- Direct and Indirect connectivity achieve similar performance in MI, being indirect connectivity less sensitive to the VC [Cao et al., 2022b]

Feature Extraction from FC

- FC feature extraction
  - Common spatial patterns
    - Constant regularization [Park et al., 2017]
      $\hat{\mathbf{C}} = \{\mathbf{C} + \alpha\mathbf{I}\}$
    - Lasso - L_1-norm [Zhang et al., 2018a]
      $\arg\max \mathbf{W}\mathbf{C}\mathbf{W}^\top - \sum_c \|\mathbf{w_c}\|_1$
    - Tikhonov L_2-norm [Fauzi et al., 2019]
      $\arg\max \mathbf{W}\mathbf{C}\mathbf{W}^\top - \sum_c \|\mathbf{w_c}\|_2$
    - Elastic-net - L_1, L_2-norm [Gu et al., 2021]
      $\arg\max \mathbf{W}\mathbf{C}\mathbf{W}^\top - \sum_c \|\mathbf{w_c}\|_1 - \sum_c \|\mathbf{w_c}\|_2$
    - Weighted regularization [Deng et al., 2020]
      $\hat{\mathbf{C}} = \{\mathbf{C} + diag(\mathbf{A})\}$
    - $L_{q/p}$ regularization [Cai et al., 2021]
      $\arg\max \mathbf{W}\mathbf{C}\mathbf{W}^\top - \sum_c \|\mathbf{w_c}\|_{p,q}$
    - Easy interpretability [Akuthota et al., 2023]
    - Easy implementation with decent performance [Khademi et al., 2023]
    - Usually $\mathbf{C}$ is calculated as the sample covariance matrix [Guo et al., 2020]
    - Ignores nonlinear interations [Ghanbar et al., 2021]
    - Not design for muti-class scenarios [Alizadeh et al., 2023]
  - Vector representation [Meng et al., 2023, Georgiadis et al., 2018]
    - CSP-like when followed by linear classification [Reuderink et al., 2011]
    - Frequently exhibit poor performance [Xu et al., 2020]
    - Easy integration with deep learning [Zoumpourlis & Patras, 2022]
  - Graph measures [Gu et al., 2023]
    - Intuitive representation [Rodrigues et al., 2022]
    - Oversimplified the cognitives process [Gonzalez-Astudillo et al., 2020]
  - Riemannian geometry [Ding et al., 2023]
    - Take into account $\mathbf{C}$ iner-links [Liu et al., 2024]
    - Hard to find best $\mathbf{C}_{ref}$ [Miah et al., 2020]
  - Topological representation [Altaheri et al., 2023, Collazos-Huertas et al., 2021]
    - Potentially lose information [Altaheri et al., 2023]
    - Performance relies on sufficient channels [Zhao et al., 2019a]
    - Seamless integration with convolutional neural networks [Xu et al., 2020b]

Outline I

Input Formulation in Deep Learning

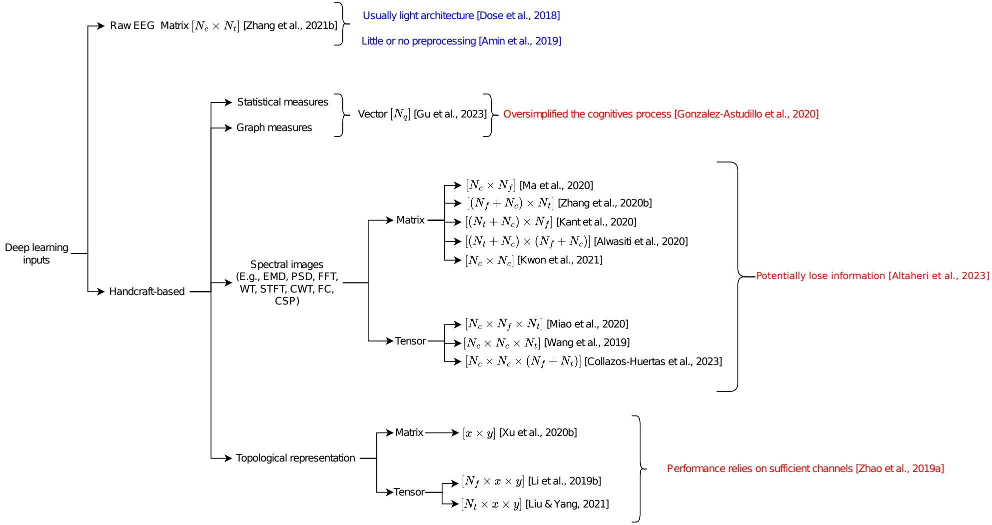

Deep Learning Architectures

- Deep learning arquitechtures
  - Discriminative Models
    - MLP [Amin et al., 2019]
      - Cannot directly extract spatial information [Altaheri et al., 2023]
    - CNN [Zhang et al., 2021c]
      - Easy to integrate with other architectures [Sharma et al., 2023]
      - Suitable for automatic spatial, temporal and spectral filtering [Köllőd et al., 2023]
    - RNN
      - LSTM [Kumar et al., 2019]
      - GRU [Luo et al., 2018]
      - Vanish gradient issue [Gao et al., 2022]
      - Inefficient in isolation [Kostiukevych et al., 2021]
    - GNN [Ju & Guan, 2023]
      - Complex model architecture [Kulatilleke, 2023]
  - Representative Models
    - DAE [Tabar & Halici, 2016]
    - DRBM [Zhang et al., 2021g]
    - DBN [Zhang et al., 2021f]
      - DBN-RBM [Xu et al., 2020b]
      - DBN-AE [Hassanpour et al., 2019]
    - Smaller datasets can lead to overfitting [Kondratyev et al., 2020]
  - Generative Models
    - VAE [Dai et al., 2019]
    - GAN [Fahimi et al., 2020]
    - Suffers from training instability [Yang et al., 2021b]

Outline I

Interpretability Strategies in MI-BCI

- XAI methods
  - Post-hoc
    - BP [Apicella et al., 2022]
    - Guided-BP [Tjoa & Guan, 2022]
      - Saturation issues [Sujatha Ravindran & Contreras-Vidal, 2023]
    - CAM [Tjoa & Guan, 2020] Cannot detect accurate locations [Lin et al., 2021]
    - Grad-CAM [Vaquerizo-Villar et al., 2023] Works with any CNN architecture [Chaddad et al., 2023] Decent accuracy location [Nunnari et al., 2021]
    - LIME [Haghanifar et al., 2022] Only linear interactions [Bramhall et al., 2020]
    - SHAP [Rashed-Al-Mahfuz et al., 2021] High time-consuming [Le et al., 2021]
    - Graph-LIME [Huang et al., 2022] Unstable explanations [Nguyen et al., 2021]
  - intrinsic Do not require external models [Wu & Mooney, 2018]

Model specific | Architecture specific | Architecture agnostic

Outline I

General Objective

To develop a single-trial indirect functional connectivity framework, accompanied by regularized deep learning approaches, to extract pertinent subject-specific non-linear spatio-temporal-frequency patterns from non-stationary EEG data, improving the MI-BCI system's accuracy and interpretability.

Specific Objectives

1. To develop a single-trial indirect FC for enhanced nonlinear feature extraction, preserving the spatio-temporal-frequency interpretability while favoring the classification performance in MI-BCI and avoiding spurious connectivities.

2. To extend the proposed single-trial FC within a deep learning scheme that handles artifacts and EEG representations, necessitating minimal preprocessing efforts from raw signals.

3. To develop a transparency and interpretability strategy dedicated to MI-BCI classification that emphasizes spatial-temporal-spectral pattern domains, incorporating a qualitative and quantitative relevance analysis assessment.

Outline I

Outline and contributions

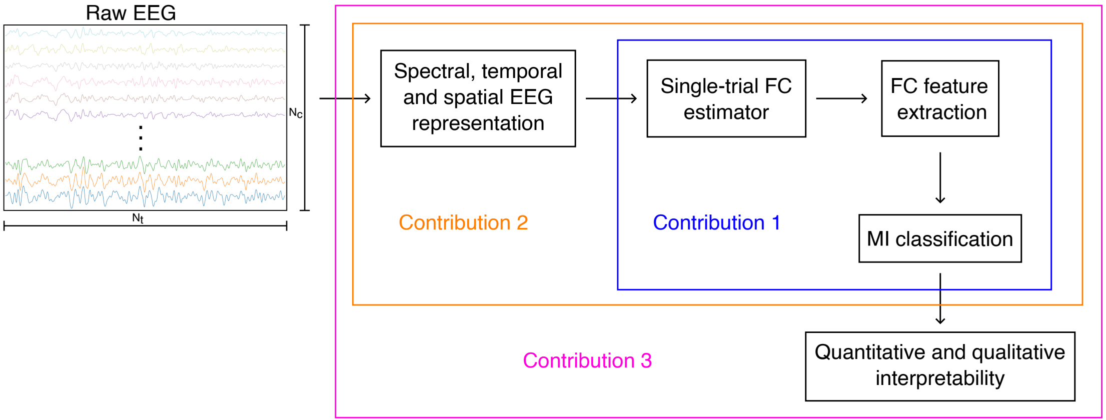

Outline I

Datasets

Dataset	Subjects	Trials	Paradigm	Classes	Channels	Sampling rate
BCI Competition IV Dataset IIa (DBI MI) [1]	9	288	Motor imagery	2	22	250Hz
Gamma Motor Execution Database (DBII ME) [2]	14	260	Motor execution	2	44	500Hz
MI BCI EEG Giga Science Database (DBIII MI) [3]	50	200	Motor imagery	2	64	500Hz

DBI MI

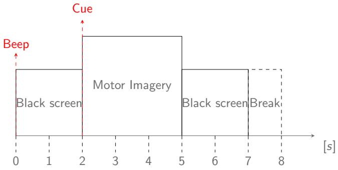

DBII ME

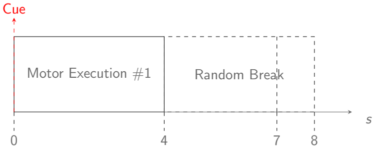

DBIII MI

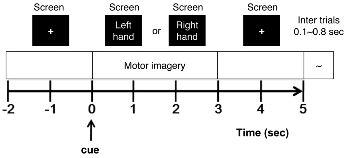

[1] http://www.bbci.de/competition/iv
[2] https://gin.g-node.org/robintibor/high-gamma-dataset
[3] http://gigadb.org/dataset/100295

Outline II

Outline II

Single-Trial Kernel-based Functional Connectivity I

1. **Wiener-Khinchin's theorem:**

$$R_r^c(\tau) = \int_{\varpi \in \Omega} \exp(j2\pi\tau\varpi)\, dP_r^c(\varpi),$$

where $P_r^c(\varpi) \in \mathbb{R}[0,1]$ is the spectral distribution function.

2. **Bochner's theorem:**

$$\kappa_r^{cc'}(\Delta_x) = \int_{\varpi \in \Omega} \exp(j2\pi\Delta_x\varpi) S_r^{cc'}(\varpi)\, d\varpi,$$

where $\Delta_x = \mathbf{x}_r^c - \mathbf{x}_r^{c'}$ is the vector delay, $\varpi \subseteq \Omega$ is the frequency domain that contains the bandwidth set of analysis Ω, and $S_r^{cc'}(\varpi)$ is the cross-spectral density.

Single-Trial Kernel-based Functional Connectivity II

3. **Cross-spectral distribution:**

$$P_r^{cc'}(\varpi) = 2\int_{\varpi\in\Omega} \mathscr{F}\left\{\kappa(\mathbf{x}_r^c, \mathbf{x}_r^{c'})\right\} d\varpi,$$

where the notation $\mathscr{F}\{\cdot\}$ stands for the Fourier transform.

4. **Kernel-based spectral distribution estimation:**

$$\hat{P}_r^{cc'}(\mathbf{u}^{cc'}, \kappa_X(\cdot;\sigma)) = \sum_{n=1}^{N_f}\sum_{w_t=1}^{N_t} u_{nw_t}^{cc'} \kappa_X\left(\mathbf{x}_{rnw_t}^{c}, \mathbf{x}_{rnw_t}^{c'};\sigma\right),$$

where $\mathbf{u}^{cc'} \in \mathbb{R}^{N_f N_t}$ is the spatio-temporal-frequency relevance vector.

Single-Trial Kernel-based Functional Connectivity III

5 **Optimization Formulation:**

$$\mathbf{u}^* = \arg\min_{\mathbf{u}} \left\langle \sum_{r=1}^{R} \left\| \sum_{c,c'=1}^{N_c} \hat{P}_r^{cc'}(\mathbf{u}^{cc'}, \kappa_x(\cdot;\sigma)) - y_r \right\|_2^2 \right\rangle + \alpha \sum_{c,c'=1}^{N_c} \|\mathbf{u}^{cc'}\|_1 + \frac{1-\alpha}{2} \sum_{c,c'=1}^{N_c} \|\mathbf{u}^{cc'}\|_2 \quad : \forall c < c',$$

where $\alpha \in \mathbb{R}^+$ is the regularization hyperparameter, y_r is the label corresponding to the r-th trial, and $\|\cdot\|_q$ is the ℓ_q-norm.

Single-Trial Kernel-based Functional Connectivity proposal

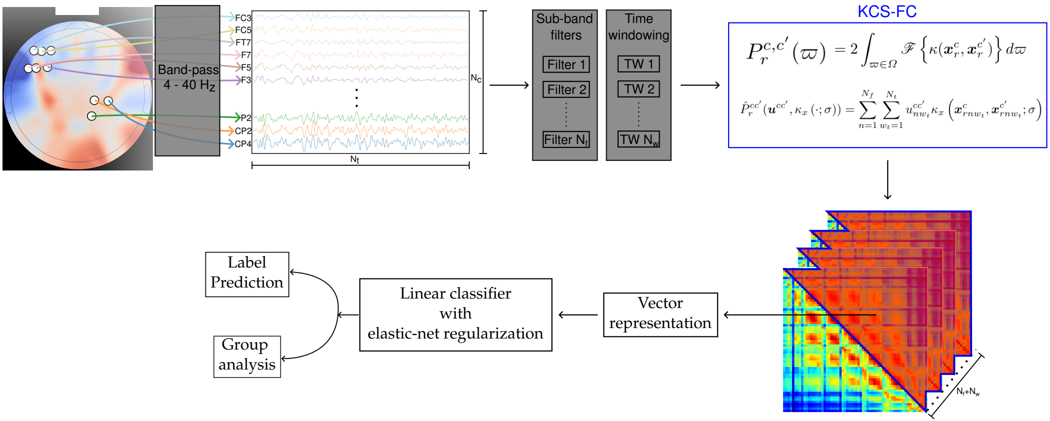

Experimental set-up

1. Sliding window of length $\tau = [0.5, 1.0, 1.5, 2.0]$ s, and overlap of 75%.
2. Frequency bands from 4 Hz to 40 Hz, window bandwidth of 4Hz, and overlap of 50%.
3. Gaussian kernel

$$\kappa_X\left(\mathbf{x}^c_{rnw_t}, \mathbf{x}^{c'}_{rnw_t}; \sigma\right) = \exp\left(-\|\mathbf{x}^c_{rnw_t} - \mathbf{x}^{c'}_{rnw_t}\|_2^2/2\sigma^2\right),$$

4. We compare our proposal with Cross-Correlation Coefficient (CCF) and Phase Lag Value (PLV)

$$\rho(\mathbf{x}^c_{rnw_t}, \mathbf{x}^{c'}_{rnw_t}) = \left\langle \mathbf{x}^c_{rnw_t}, \mathbf{x}^{c'}_{rnw_t} \right\rangle$$

$$\Delta\phi(\mathbf{x}^c_{rnw_t}, \mathbf{x}^{c'}_{rnw_t}) = |\exp(j(\phi^c_{rnw_t} - \phi^{c'}_{rnw_t}))|$$

Impact of Prior CSP Filtering

- PLV shows high variance and low accuracy..
- KCS-FC outperforms other FC measures, with less variance in accuracy across subjects.
- CSP accuracy drops at $\tau = 0.5$ due to its reliance on FC estimation, with less information leading to poorer estimates.

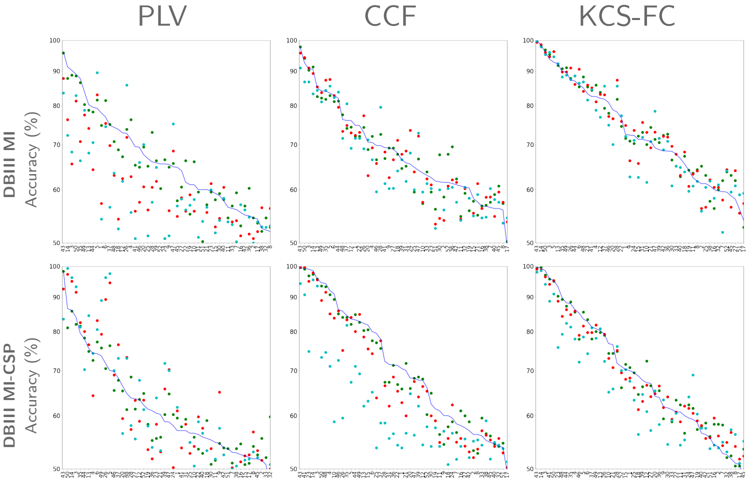

Influence of Sliding Windows

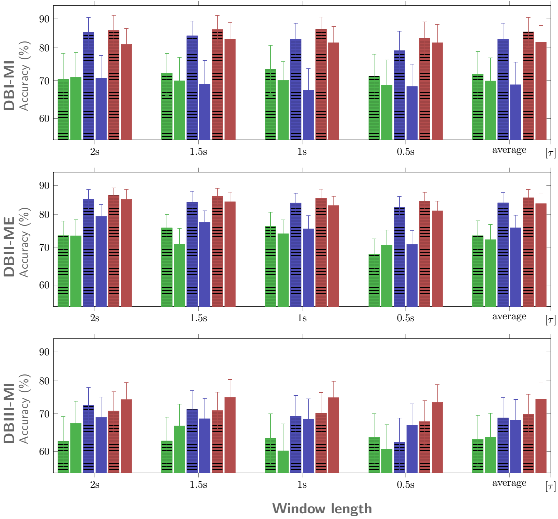

Classifier Accuracy of Individuals I

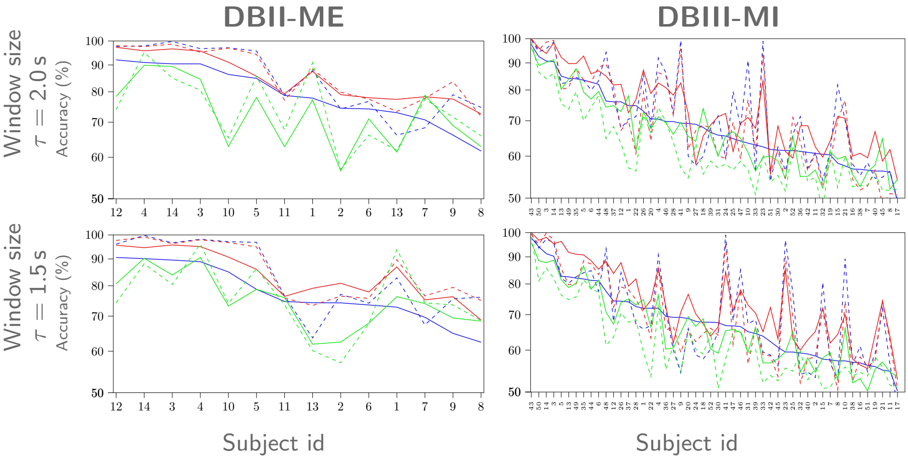

Classifier Accuracy of Individuals II

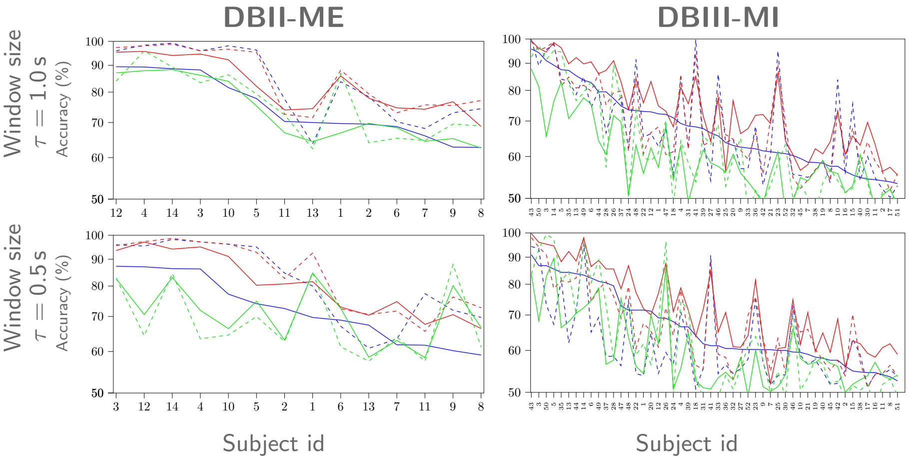

Interpretation of Subject Clusters

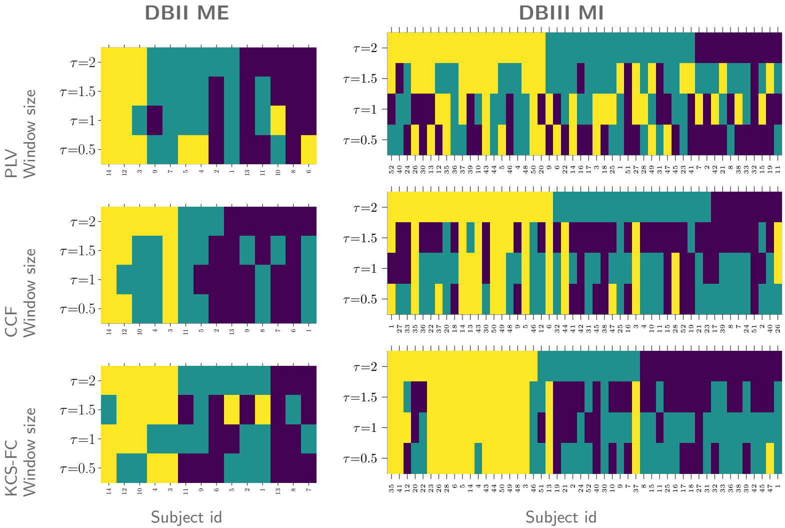

asd

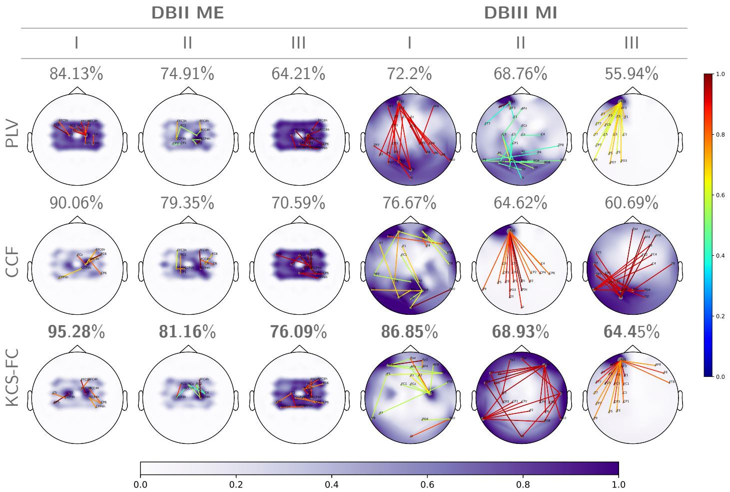
DBII ME
DBIII MI
I
II
III
I
II
III
84.13%
74.91%
64.21%
72.2%
68.76%
55.94%
PLV
90.06%
79.35%
70.59%
76.67%
64.62%
60.69%
CCF
95.28%
81.16%
76.09%
86.85%
68.93%
64.45%
KCS-FC
0.0
0.2
0.4
0.6
0.8
1.0

Classifier accuracy comparison of FC approaches

Data	Time Window	Filter Band	Interpretation	Feature Extraction	Accuracy (%)
DBI-MI	✓	✓	✓	TSGSP [Zhang et al., 2018]	**82.50** $\pm$ **12.2**
	-	-	✓	STR connectivity [Rodrigues et al., 2019]	69.56$\pm$15.02
	✓	-	✓	Renyi's α-entropy [De La Pava Panche et al., 2019]	72.40 $\pm$ 6.50
	✓	✓	✓	Proposed KCS-FC	81.92 $\pm$ 9.44
DBIII-MI	-	✓	✓	CSP [Cho et al., 2017]	67.60 $\pm$ 13.17
	✓	✓	-	OPTICAL [Kumar et al., 2019]	68.19 $\pm$ 9.36
	-	-	✓	STR connectivity [Rodrigues et al., 2019]	62.00 $\pm$ 13.00
	✓	✓	✓	Proposed KCS-FC	**74.12** $\pm$ **12.13**

Outline II

Kernel Cross-Spectral Functional Connectivity Network I

1. **1-D convolutional feature extraction and Gaussian pairwise similarity:**

$$\hat{\boldsymbol{P}}_r(\boldsymbol{w}_f) = \tilde{K}(\cdot;\sigma) \circ \varphi(\boldsymbol{X}_r; \boldsymbol{w}_f),$$

where $\tilde{K}(\tilde{\boldsymbol{X}}_r;\sigma) = [\boldsymbol{K}_{r1}, \boldsymbol{K}_{r2}, \cdots, \boldsymbol{K}_{rf}, \cdots, \boldsymbol{K}_{rN_f}]$ and $\boldsymbol{K}_{rf}$ is defined as:

$$\boldsymbol{K}_{rf} = \begin{bmatrix} \kappa_X(\boldsymbol{x}_{rf}^1, \boldsymbol{x}_{rf}^1;\sigma) & \kappa_X(\boldsymbol{x}_{rf}^1, \boldsymbol{x}_{rf}^2;\sigma) & \cdots & \kappa_X(\boldsymbol{x}_{rf}^1, \boldsymbol{x}_{rf}^{N_c};\sigma) \\ \kappa_X(\boldsymbol{x}_{rf}^2, \boldsymbol{x}_{rf}^1;\sigma) & \kappa_X(\boldsymbol{x}_{rf}^2, \boldsymbol{x}_{rf}^2;\sigma) & \cdots & \kappa_X(\boldsymbol{x}_{rf}^2, \boldsymbol{x}_{rf}^{N_c};\sigma) \\ \vdots & \vdots & \ddots & \vdots \\ \kappa_X(\boldsymbol{x}_{rf}^{N_c}, \boldsymbol{x}_{rf}^1;\sigma) & \kappa_X(\boldsymbol{x}_{rf}^{N_c}, \boldsymbol{x}_{rf}^2;\sigma) & \cdots & \kappa_X(\boldsymbol{x}_{rf}^{N_c}, \boldsymbol{x}_{rf}^{N_c};\sigma). \end{bmatrix}$$

2. **Average functional connectivity measure:**

$$\tilde{\boldsymbol{P}}_r = \mathrm{AvgPooling}_f \left(\hat{\boldsymbol{P}}_r(\boldsymbol{w}_f)\right),$$

Kernel Cross-Spectral Functional Connectivity Network II

3. **Vectorized version of $\tilde{P}_r$:**

$$\overline{\boldsymbol{p}}_r = \left[\tilde{p}_r^{12}, \tilde{p}_r^{13}, \cdots, \tilde{p}_r^{cc'}, \cdots, \tilde{p}_r^{(N_c-1)N_c}\right]; \forall c < c',$$

4. **Optimization Formulation:**

$$\Theta^* = \arg\min_{\Theta} \quad \mathbb{E}_r\{\mathcal{L}(\boldsymbol{y}_r, \hat{\boldsymbol{y}}_r|\Theta); \forall r \in \{1, 2, \ldots, R\}\},$$

where $\mathcal{L}\{\cdot\}$ is a given loss function, and $\hat{\boldsymbol{y}}_r = \mathrm{softmax}\left(\boldsymbol{V}\overline{\boldsymbol{p}}_r + \boldsymbol{b}\right)$

Kernel Cross-Spectral Functional Connectivity Network proposal

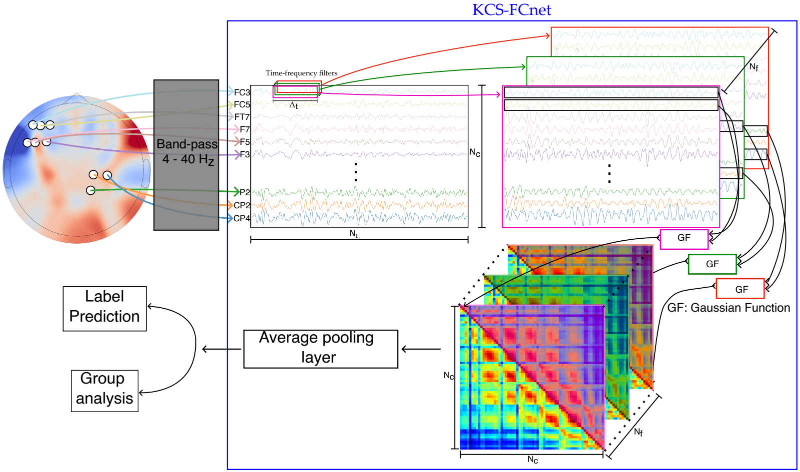

Kernel Cross-Spectral Functional Connectivity Network architecture

Layer	Output Dimension	Params.
Input	$N_c \times N_t \times 1$	·
Conv2D	$N_c \times (N_t - \Delta_t + 1) \times N_f$	max norm = 2.0, kernel size = $(1, \Delta_t)$ Stride size = (1, 1), Bias = False
BatchNormalization	$N_c \times (N_t - \Delta_t + 1) \times N_f$	·
	ELU activation	
KCS-FCblock	$N_f \times (N_c \cdot (N_c - 1)/2) \times 1$	·
AveragePooling2D	$1 \times (N_c \cdot (N_c - 1)/2) \times 1$	·
BatchNormalization	$1 \times (N_c \cdot (N_c - 1)/2) \times 1$	·
	ELU activation	
Flatten	$N_c \cdot (N_c - 1)/2$	·
Dropout	$N_c \cdot (N_c - 1)/2$	Dropout rate = 0.5
Dense	N_y	max norm = 0.5
	Softmax	

Experimental set-up

1. **Raw EEG Preprocessing:**
   - Database used DBIII MI
   - Donwsampling from 512 Hz to 128 Hz.
   - Filtering from 4 Hz to 40 Hz.
   - Records clipped from 0.5 s to 2.5 s post cue.
2. **KCS-FCnet Training:**
   - Data split using 5-fold 80-20 scheme.
   - 1-D convolutional kernel length set to 20 as in [Lawhern et al., 2018]
   - Number of filters were searched within the set $\{2, 3, 4\}$
3. **Group-Level Analysis:**
   - Scaled scoring matrix with subjects and accuracy, Cohen's kappa, AUC.
   - Cluster subjects in three groups based on base line EEGnet.
   - PCA was used to reduce the dimensions to two, enabling us to plot it.

Subject Dependent and Group Analysis Results I

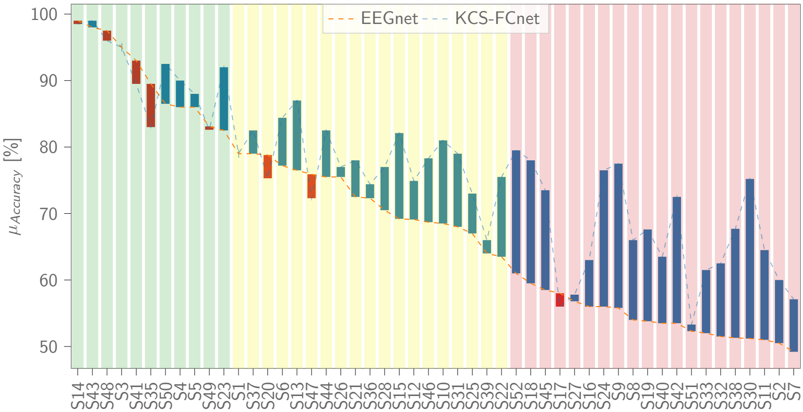

Subject Dependent and Group Analysis Results II

Subject Dependent and Group Analysis Results III

Approach	Group	Accuracy	KCS-FCnet Gain
EEGnet	G I	90.6 ± 4.3	·
	G II	72.2 ± 7.3	·
	G III	54.3 ± 6.6	·
KCS-FCnet	G I	91.5 ± 3.3	**0.9**
	G II	77.8 ± 4.7	**5.6**
	G III	66.7 ± 5.6	**12.4**

Subject Dependent and Group Analysis Results IV

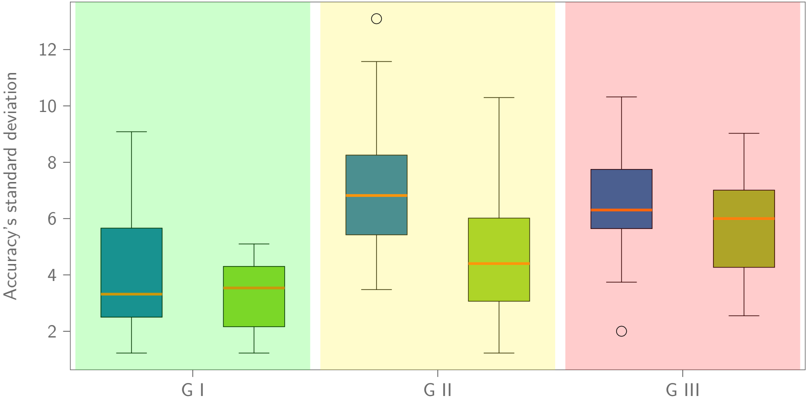

Functional connectivity analysis I

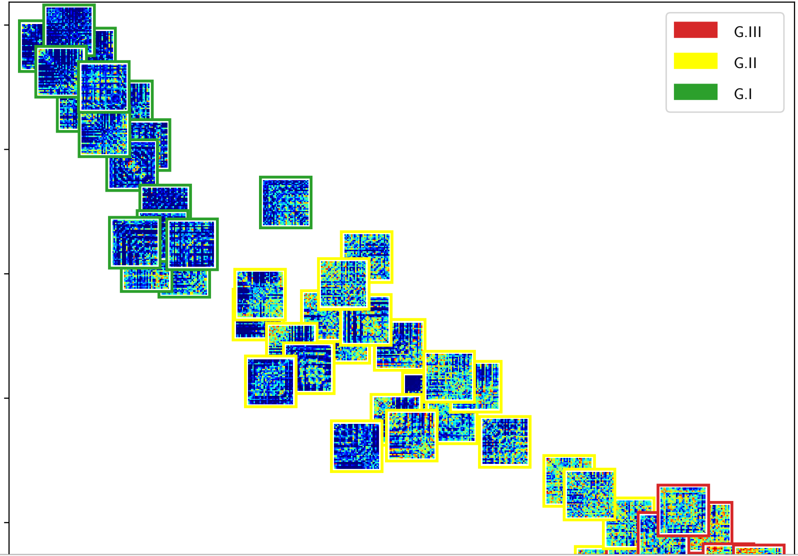

Functional connectivity analysis II

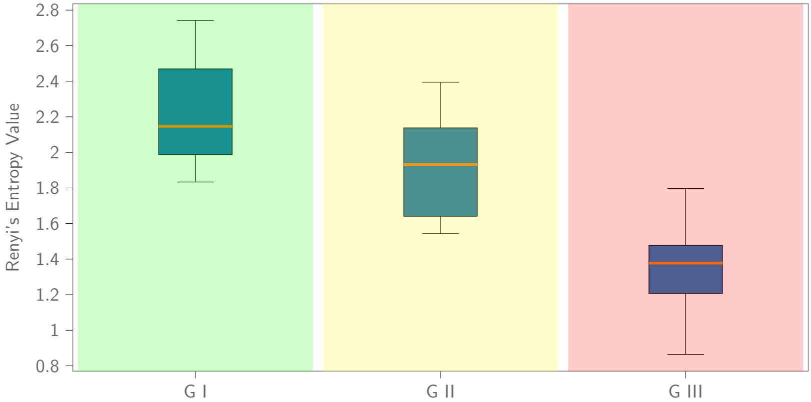

Functional connectivity analysis III

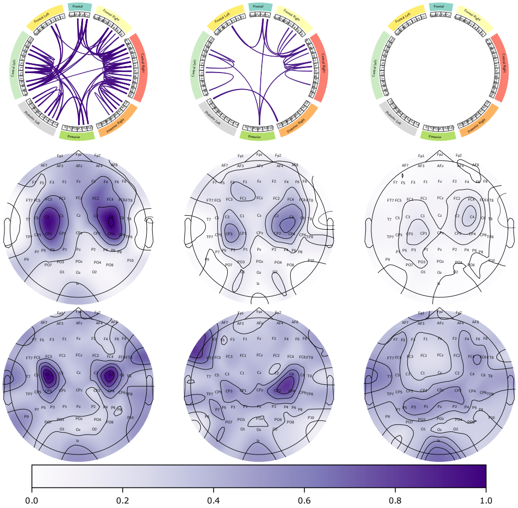

Classifier accuracy comparison of DL approaches I

Approach	Accuracy	Kappa	AUC
Deepconvnet [Schirrmeister et al., 2017]	62.5 ± 13.0	24.5 ± 25.9	68.9 ± 17.8
EEGnet [Lawhern et al., 2018]	69.0 ± 14.6	38.0 ± 29.1	75.4 ± 16.6
TCNet-Fusion [Musallam et al., 2021]	72.7 ± 14.0	45.0 ± 28.2	79.6 ± 15.9
Shallowconvnet [Schirrmeister et al., 2017]	74.9 ± 13.9	49.5 ± 27.8	79.9 ± 15.1
KCS-FCnet	76.4 ± 11.3	52.6 ± 22.7	82.2 ± 12.2

Classifier accuracy comparison of DL approaches II

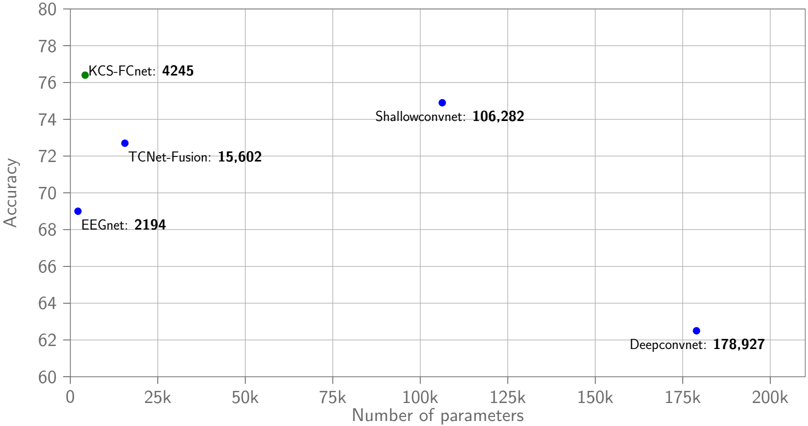

Outline II

Interpretable regularized kernel cross-spectral FC network I

1. **Parzen density estimation:**

$$\hat{\zeta}(\chi) = \frac{1}{N_c} \sum_{c=1}^{N_c} \kappa(\chi, x^c; \sigma),$$

2. **Renyi's entropy $\alpha = 2$:**

$$\begin{aligned} H_2(\chi) &= -\log\left(\int_{\chi} \hat{\zeta}(\chi)^2 \, d\zeta\right) \\ &= -\log\left(\frac{1}{N_c^2} \sum_{c,c'=1}^{N_c} \kappa(\boldsymbol{x}^c, \boldsymbol{x}^{c'}; \sigma)\right). \end{aligned}$$

Interpretable regularized kernel cross-spectral FC network II

3. **Concept extended to function composition:**

$$\hat{\zeta}(\chi) = \frac{1}{N_c}\sum_{c=1}^{N_c} \kappa_X(\chi, \cdot; \sigma) \circ \varphi(\boldsymbol{x}^c; \boldsymbol{w}_f),$$

where $\varphi(\cdot; \boldsymbol{w}_f)$ is a 1-D convolutional layer.

4. **Optimization Formulation with cross-information potential regularization:**

$$\Theta^* = \arg\min_{\Theta} \quad \mathbb{E}_r\{R\}\left[\mathcal{L}(\boldsymbol{y}_r, \hat{\boldsymbol{y}}_r|\Theta) - H(\tilde{\boldsymbol{P}}_r; \boldsymbol{w}_f, \sigma)\right]; \forall r \in \{1, 2, \ldots, R\},$$

where

$$H(\tilde{\boldsymbol{P}}_r; \boldsymbol{w}_f, \sigma) = -\log\left(\frac{1}{N_c^2}\sum_{c,c'=1}^{N_c} \kappa_X(\cdot, \cdot; \sigma) \circ \left(\tilde{p}_r^{c'}(\boldsymbol{w}_f), \tilde{p}_r^{c}(\boldsymbol{w}_f)\right)\right).$$

Interpretable regularized kernel cross-spectral FC network proposal

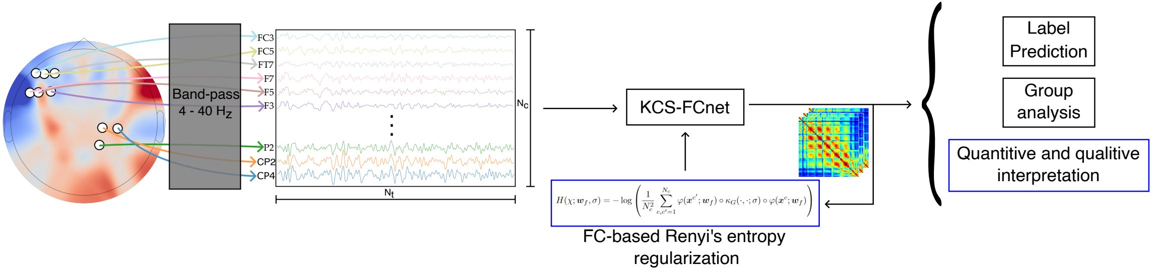

Experimental set-up

1. **Raw EEG Preprocessing:**
   - Database used DBIII MI
   - Donwsampling from 512 Hz to 128 Hz.
   - Filtering from 4 Hz to 40 Hz.
   - Records clipped from 0.5 s to 2.5 s post cue.
2. **KCS-FCnet Training:**
   - Data split using 5-fold 80-20 scheme.
   - 1-D convolutional kernel length set to 20 as in [Lawhern et al., 2018]
   - Number of filters were taken from the best results within the original model
3. **Group-Level Analysis:**
   - Scaled scoring matrix with subjects and accuracy, Cohen's kappa, AUC.
   - Cluster subjects in three groups absed on base line EEGnet.
   - PCA was used to reduce the dimensions to two, enabling us to plot it.

Model level analysis I

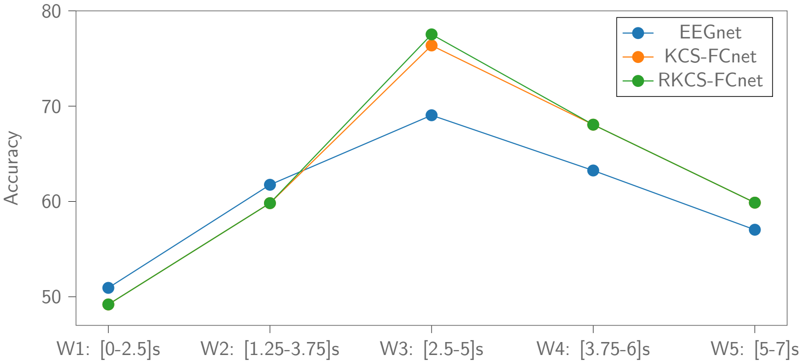

Model level analysis II

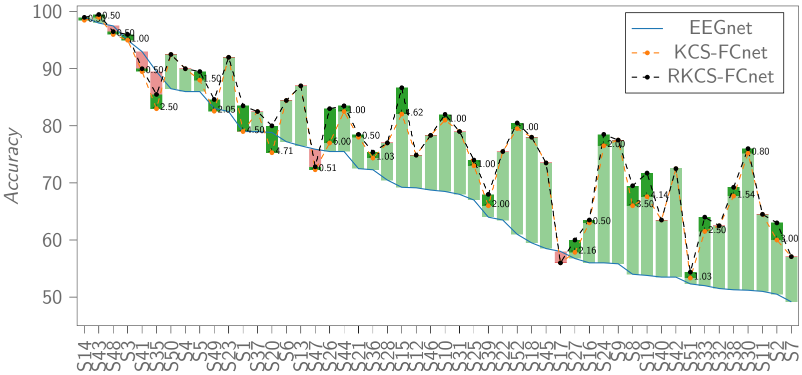

Group level analysis I

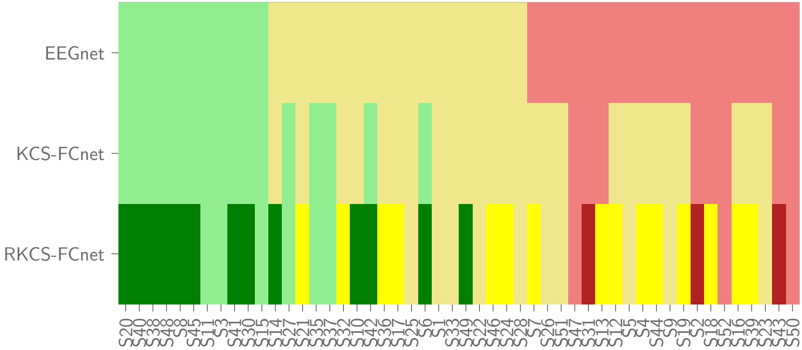

Group level analysis II

Strategy	G I	G II	G III
EEGnet	90.55 ± 5.88	72.15 ± 4.87	54.27 ± 3.21
KCS-FCnet	91.46 ± 5.31	77.85 ± 4.76	66.66 ± 7.88
IRKCS-FCnet	**92.28 ± 4.79**	**79.26 ± 4.93**	**67.77± 7.83**

Group level analysis III

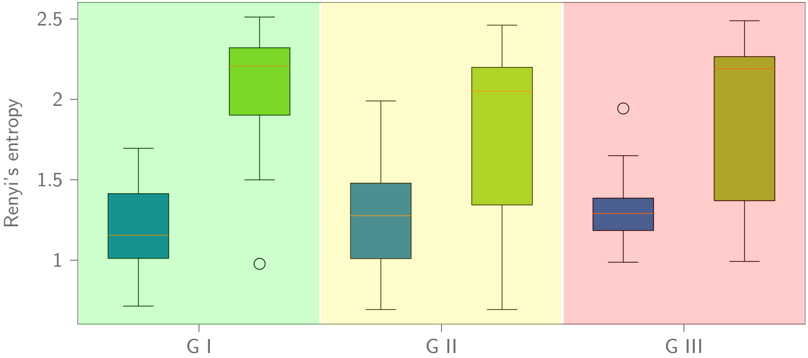

Post-hoc interpretability

Group	KCS-FCnet vs. Random	RKCS-FCnet vs. Random
G I	0.00077*	0.00230*
G II	0.00368*	0.00434*
G III	0.00108*	0.00074*

Strategy	Group	25%	20%	15%	10%	5%
KCS-FCnet	G I	40.51	37.93	35.97	30.25	17.12
	G II	40.10	39.00	36.46	28.60	17.72
	G III	39.05	36.98	31.99	25.28	15.02
RKCS-FCnet	G I	44.80	39.21	37.79	30.55	22.46
	G II	41.08	40.01	36.77	27.28	18.84
	G III	39.65	37.30	33.12	27.10	16.80

Intrinsic interpretability I

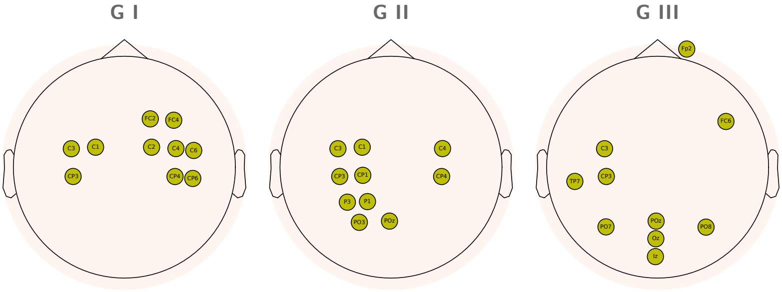

Intrinsic interpretability II

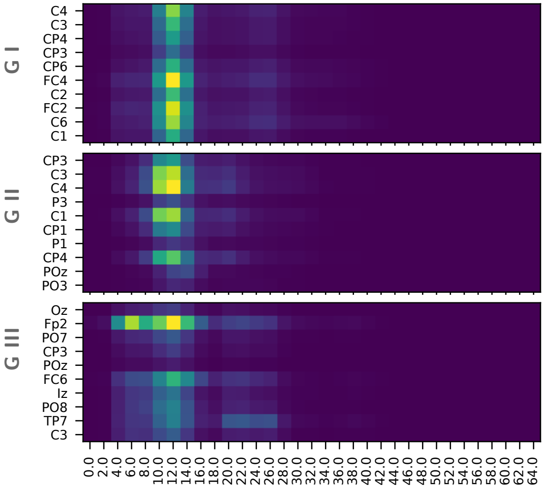

Intrinsic interpretability III

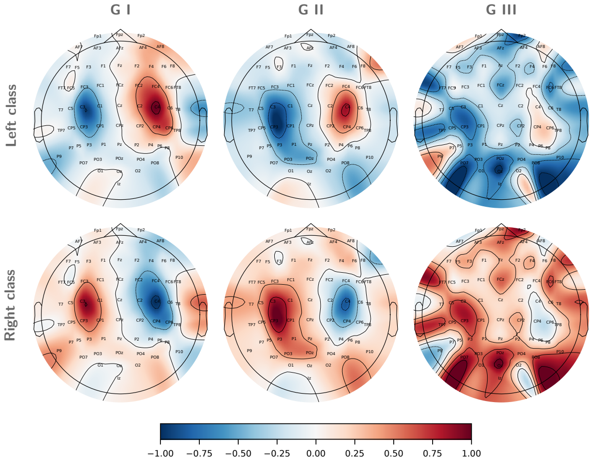

Individual subject analysis I

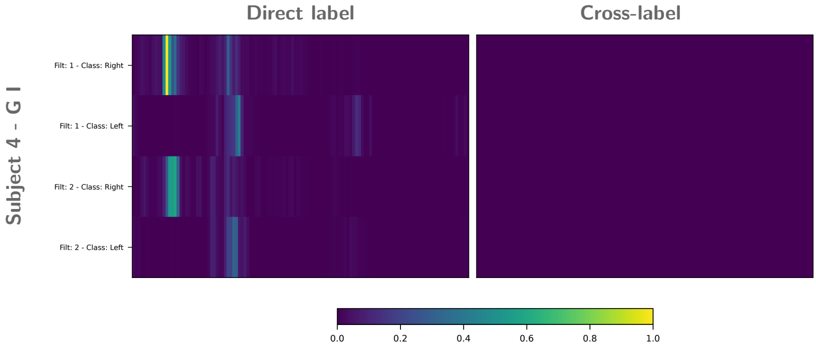

Individual subject analysis II

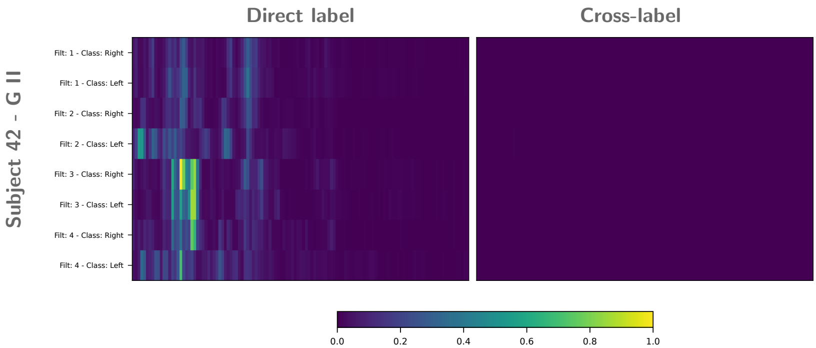

Individual subject analysis III

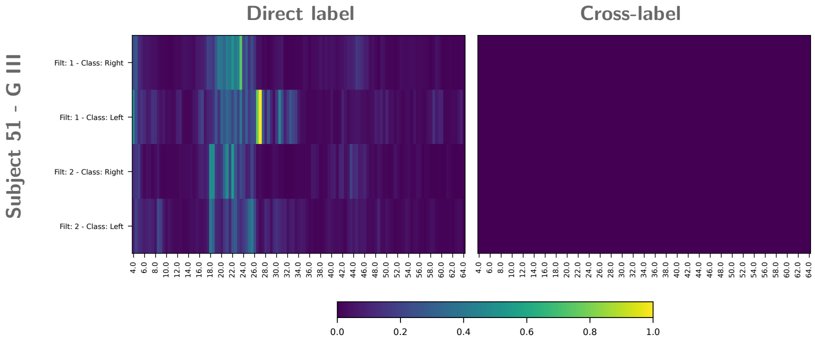

Outline II

Conclusions

- conclusions

Outline II

Future work

- Future work

Outline II

References I

Ahn, M., Lee, M., Choi, J., and Jun, S. C. (2014).
A review of brain-computer interface games and an opinion survey from researchers, developers and users.
Sensors, 14(8):14601–14633.

Ai, Q., Chen, A., Chen, K., Liu, Q., Zhou, T., Xin, S., and Ji, Z. (2019).
Feature extraction of four-class motor imagery EEG signals based on functional brain network.
Journal of Neural Engineering, 16(2):026032.

Alsharif, A., Salleh, N., Baharun, R., and Safaei, M. (2020).
Neuromarketing approach: An overview and future research directions.
Journal of Theoretical and Applied Information Technology, 98(7):991–1001.

Altaheri, H., Muhammad, G., Alsulaiman, M., Amin, S. U., Altuwaijri, G. A., Abdul, W., Bencherif, M. A., and Faisal, M. (2023).
Deep learning techniques for classification of electroencephalogram (eeg) motor imagery (mi) signals: A review.
Neural Computing and Applications, 35(20):14681–14722.

Barios, J. A., Ezquerro, S., Bertomeu-Motos, A., Nann, M., Badesa, F. J., Fernandez, E., Soekadar, S. R., and Garcia-Aracil, N. (2019).
Synchronization of slow cortical rhythms during motor imagery-based brain–machine interface control.
International journal of neural systems, 29(05):1850045.

Bonci, A., Fiori, S., Higashi, H., Tanaka, T., and Verdini, F. (2021).
An introductory tutorial on brain–computer interfaces and their applications.
Electronics, 10(5):560.

References II

Cao, J., Zhao, Y., Shan, X., Wei, H.-l., Guo, Y., Chen, L., Erkoyuncu, J. A., and Sarrigiannis, P. G. (2022a).
Brain functional and effective connectivity based on electroencephalography recordings: A review.
Human brain mapping, 43(2):860–879.

Cao, L., Wang, W., Huang, C., Xu, Z., Wang, H., Jia, J., Chen, S., Dong, Y., Fan, C., and de Albuquerque, V. H. C. (2022b).
An effective fusing approach by combining connectivity network pattern and temporal-spatial analysis for eeg-based bci rehabilitation.
IEEE Transactions on Neural Systems and Rehabilitation Engineering, 30:2264–2274.

Casimo, K., Weaver, K. E., Wander, J., and Ojemann, J. G. (2017).
Bci use and its relation to adaptation in cortical networks.
IEEE Transactions on Neural Systems and Rehabilitation Engineering, 25(10):1697–1704.

Cattan, G., Mendoza, C., Andreev, A., and Congedo, M. (2018).
Recommendations for integrating a p300-based brain computer interface in virtual reality environments for gaming.
Computers, 7(2):34.

Chevallier, S., Carrara, I., Aristimunha, B., Guetschel, P., Sedlar, S., Lopes, B., Velut, S., Khazem, S., and Moreau, T. (2024).
The largest eeg-based bci reproducibility study for open science: the moabb benchmark.
arXiv preprint arXiv:2404.15319.

Chiarion, G., Sparacino, L., Antonacci, Y., Faes, L., and Mesin, L. (2023).
Connectivity analysis in eeg data: A tutorial review of the state of the art and emerging trends.
Bioengineering, 10(3):372.

References III

Cho, H., Ahn, M., Ahn, S., Kwon, M., and Jun, S. (2017).
EEG datasets for motor imagery brain–computer interface.
GigaScience, 6(7):gix034.

Collazos-Huertas, D. F., Álvarez-Meza, A. M., Cárdenas-Peña, D. A., Castaño-Duque, G. A., and Castellanos-Domínguez, C. G. (2023).
Posthoc interpretability of neural responses by grouping subject motor imagery skills using cnn-based connectivity.
Sensors, 23(5):2750.

De La Pava Panche, I., Alvarez-Meza, A., and Orozco-Gutierrez, A. (2019).
A data-driven measure of effective connectivity based on renyi's α-entropy.
Frontiers in neuroscience, 13:1277.

Gonzalez-Astudillo, J., Cattai, T., Bassignana, G., Corsi, M.-C., and Fallani, F. D. V. (2020).
Network-based brain computer interfaces: principles and applications.
Journal of Neural Engineering.

Grigorev, N. A., Savosenkov, A. O., Lukoyanov, M. V., Udoratina, A., Shusharina, N. N., Kaplan, A. Y., Hramov, A. E., Kazantsev, V. B., and Gordleeva, S. (2021).
A bci-based vibrotactile neurofeedback training improves motor cortical excitability during motor imagery.
IEEE Transactions on Neural Systems and Rehabilitation Engineering, 29:1583–1592.

Hamedi, M., Salleh, S.-H., Noor, A. M., and Mohammad-Rezazadeh, I. (2014).
Neural network-based three-class motor imagery classification using time-domain features for bci applications.
In *2014 IEEE region 10 symposium*, pages 204–207. IEEE.

References IV

He, B., Astolfi, L., Valdés-Sosa, P. A., Marinazzo, D., Palva, S. O., Bénar, C.-G., Michel, C. M., and Koenig, T. (2019).
Electrophysiological brain connectivity: theory and implementation.
IEEE Transactions on Biomedical Engineering, 66(7):2115–2137.

Hosseini, M.-P., Hosseini, A., and Ahi, K. (2020).
A review on machine learning for EEG signal processing in bioengineering.
IEEE reviews in biomedical engineering.

Janapati, R., Dalal, V., and Sengupta, R. (2023).
Advances in modern eeg-bci signal processing: A review.
Materials Today: Proceedings, 80:2563–2566.

Khan, M. A., Das, R., Iversen, H. K., and Puthusserypady, S. (2020).
Review on motor imagery based BCI systems for upper limb post-stroke neurorehabilitation: From designing to application.
Computers in Biology and Medicine, page 103843.

Kumar, S., Sharma, A., and Tsunoda, T. (2019).
Brain wave classification using long short-term memory network based OPTICAL predictor.
Scientific reports, 9(1):1–13.

Lawhern, V. J., Solon, A. J., Waytowich, N. R., Gordon, S. M., Hung, C. P., and Lance, B. J. (2018).
Eegnet: a compact convolutional neural network for eeg-based brain–computer interfaces.
Journal of neural engineering, 15(5):056013.

References V

Li, S., Xie, X., Gu, Z., Yu, Z. L., and Li, Y. (2019).
Motor imagery classification based on local isometric embedding of riemannian manifold.
In *2019 14th IEEE Conference on Industrial Electronics and Applications (ICIEA)*, pages 2368–2372. IEEE.

Musallam, Y. K., AlFassam, N. I., Muhammad, G., Amin, S. U., Alsulaiman, M., Abdul, W., Altaheri, H., Bencherif, M. A., and Algabri, M. (2021).
Electroencephalography-based motor imagery classification using temporal convolutional network fusion.
Biomedical Signal Processing and Control, 69:102826.

Oikonomou, V. P., Georgiadis, K., Liaros, G., Nikolopoulos, S., and Kompatsiaris, I. (2017).
A comparison study on eeg signal processing techniques using motor imagery eeg data.
In *2017 IEEE 30th international symposium on computer-based medical systems (CBMS)*, pages 781–786. IEEE.

Purves, W. K. (c 2001.).
Life, the science of biology /.
Sinauer Associates,, Sunderland, MA :, 6th ed. edition.
Includes index.

Rodrigues, P., Stefano, C., Attux, R., Castellano, G., and Soriano, D. (2019).
Space-time recurrences for functional connectivity evaluation and feature extraction in motor imagery brain-computer interfaces.
Medical & biological engineering & computing, 57(8):1709–1725.

Roy, G., Bhoi, A., and Bhaumik, S. (2022).
A comparative approach for mi-based eeg signals classification using energy, power and entropy.
IRBM, 43(5):434–446.

References VI

Samuel, O. W., Geng, Y., Li, X., and Li, G. (2017).
Towards efficient decoding of multiple classes of motor imagery limb movements based on eeg spectral and time domain descriptors.
Journal of medical systems, 41:1–13.

Sarraf, S. (2017).
Eeg-based movement imagery classification using machine learning techniques and welch's power spectral density estimation.
American Scientific Research Journal for Engineering, Technology, and Sciences (ASRJETS), 33(1):124–145.

Schirrmeister, R. T., Springenberg, J. T., Fiederer, L. D. J., Glasstetter, M., Eggensperger, K., Tangermann, M., Hutter, F., Burgard, W., and Ball, T. (2017).
Deep learning with convolutional neural networks for EEG decoding and visualization.
Human brain mapping, 38(11):5391–5420.

Singh, A., Hussain, A. A., Lal, S., and Guesgen, H. W. (2021).
A comprehensive review on critical issues and possible solutions of motor imagery based electroencephalography brain-computer interface.
Sensors, 21(6):2173.

Sitaram, R., Ros, T., Stoeckel, L., Haller, S., Scharnowski, F., Lewis-Peacock, J., Weiskopf, N., Blefari, M. L., Rana, M., Oblak, E., et al. (2017).
Closed-loop brain training: the science of neurofeedback.
Nature Reviews Neuroscience, 18(2):86–100.

Thiebaut de Schotten, M., Foulon, C., and Nachev, P. (2020).
Brain disconnections link structural connectivity with function and behaviour.
Nature communications, 11(1):5094.

References VII

Vărbu, K., Muhammad, N., and Muhammad, Y. (2022).
Past, present, and future of eeg-based bci applications.
Sensors, 22(9):3331.

Yilmaz, C. M., Kose, C., and Hatipoglu, B. (2018).
A quasi-probabilistic distribution model for eeg signal classification by using 2-d signal representation.
Computer methods and programs in biomedicine, 162:187–196.

Zhang, Y., Nam, C., Zhou, G., Jin, J., Wang, X., and Cichocki, A. (2018).
Temporally constrained sparse group spatial patterns for motor imagery BCI.
IEEE transactions on cybernetics, 49(9):3322–3332.